

THE OFFICIAL MAGAZINE OF THE OCEANOGRAPHY SOCIETY

Oceanography

CITATION

Kwok, R., and D. Sulsky. 2010. Arctic Ocean sea ice thickness and kinematics: Satellite retrievals and modeling. *Oceanography* 23(4):134–143, doi:10.5670/oceanog.2010.11.

COPYRIGHT

This article has been published in *Oceanography*, Volume 23, Number 4, a quarterly journal of The Oceanography Society. Copyright 2010 by The Oceanography Society. All rights reserved.

USAGE

Permission is granted to copy this article for use in teaching and research. Republication, systematic reproduction, or collective redistribution of any portion of this article by photocopy machine, reposting, or other means is permitted only with the approval of The Oceanography Society. Send all correspondence to: info@tos.org or The Oceanography Society, PO Box 1931, Rockville, MD 20849-1931, USA.

BY RON KWOK AND DEBORAH SULSKY

Arctic Ocean Sea Ice Thickness and Kinematics

SATELLITE RETRIEVALS AND MODELING

ABSTRACT. Sea ice in the Arctic Ocean ranges from thin new ice to thick deformed ridges. Changes in thickness are due to melting and freezing, and to physical rearrangement of existing ice to form leads and pressure ridges. As a brittle solid, fractures are created when the ice cover moves and deforms. Openings along fractures are sites of local heat exchange between the atmosphere and ocean, and of local ice production in the winter as ocean water freezes when exposed to the colder atmosphere. Closing of the ice forces it to raft or pile up into pressure ridges and to be forced down into keels, increasing the volume of sea ice that can be stored within a given area of the Arctic Ocean. This mechanical redistribution of sea ice affects ice strength and has a profound impact on ice behavior over a wide range of temporal and spatial scales. Accurate observation and simulation of the relative contributions of thermodynamics and dynamics to ice thickness distribution are thus critical for understanding the ice cover in terms of how it changes, and its vulnerability in a warming climate. Recent satellite altimetry and high-resolution synthetic aperture radar imaging have provided near-basin-scale views of ice thickness and motion for use in quantifying changes, and for assessment and refinement of models. During this coming decade, several satellite missions are poised to provide improved, coordinated, and near-continuous measurements of thickness and motion that will advance our understanding of Arctic ice cover. Here, we provide an overview of our current capabilities and the future prospects for observing these parameters from space.

INTRODUCTION

The Northern Hemisphere's sea ice extent has been declining at an average rate of about 3% per decade over the satellite record (1978–present), and summer decline seems to be accelerating (Comiso et al., 2008). In September 2007, the summer ice extent reached a record minimum of $4.2 \times 10^6 \text{ km}^2$, which was $1.6 \times 10^6 \text{ km}^2$ or 23% less than the previous record set in September 2005. The loss of old, multiyear ice is occurring at an even higher rate of about 10% per decade (Comiso, 2002). In addition to these astonishing trends in Arctic summer ice coverage, recent studies show a parallel thinning of the ice cover from a winter thickness of 3.64 m to 1.89 m between 1980 and 2008, a net decrease of 1.75 m or 48% in mean ice thickness (Kwok and Rothrock, 2009). More than two-thirds of the Arctic is now covered by thinner seasonal ice. If current rates persist, the survivability of summer ice cover is in question.

Changes in Arctic ice cover are linked to global climate change. Although models agree that increased greenhouse gas concentrations will result in a reduction of Arctic sea ice area and volume, there is much uncertainty in projections of the rate at which this will occur. To further our understanding and to improve the projected behavior of the Arctic sea ice system, integrated contemporaneous observations of atmosphere/ice/ocean interactions are essential. Without such observations, it is very difficult to describe current conditions in the Arctic, let alone understand the changes that are underway, or their connections to the rest of the Earth system. Although we have seen progress, the Arctic is a region with a limited

record of observations. Past observations have been low density, with limited duration and coordination. The Arctic is a logistically challenging and cost-prohibitive environment for mounting extensive field programs. The trend in the ice extent as seen from satellites, a rather coarse indicator of ice behavior, has been monitored for only three decades (1978–present). Yet, satellite estimates of ice extent have served as our bellwether for changes in Arctic sea ice cover and polar climate. Near-basin-scale estimates of ice thickness and relatively high-resolution estimates of ice motion, which provide a more detailed but limited picture of the ice cover response to atmosphere and ocean forcing, have only recently been available. The variability and coupled behavior of Arctic sea ice thickness and kinematics, at decadal time scales, remain to be quantified. Because of the sampling requirements of these two quantities, spaceborne instruments together with field programs are indispensable components of a comprehensive system to address our observational needs (Polar Research Board, 2006; Integrated Global Observing Strategy, 2007).

In this article, we review briefly the progress and future of satellite observations of sea ice motion from high-resolution synthetic aperture radar (SAR) imagery and of ice thickness from light detection and ranging (lidar) and radar altimetry. We highlight some Arctic sea ice cover trends attributable to these observations, as well as the current and future uses of these data sets in sea ice modeling. Finally, we discuss the prospects of coordinated satellite monitoring of sea ice parameters in this coming decade.

SEA ICE KINEMATICS

Sea ice moves in response to wind and ocean currents. Large-scale circulation of sea ice (Figure 1a) determines the advective part of the ice balance (i.e., the regional exchange of sea ice and export to lower-latitude oceans). This knowledge provides a velocity boundary condition on the ocean surface, while the small-scale motion describes the interaction of individual floes, aggregation of floes, and the formation of leads (areas of open water) and ridges. In this section, we focus on the geophysical significance and the observations of small-scale sea ice motion.

The mechanical response of the ice cover to large-scale atmospheric and oceanic forcing is concentrated along fractures up to kilometers in widths, and lengths that can span thousands of kilometers. Rather than deforming continuously throughout the ice cover, sea ice moves and deforms due to fractures/cracks created by brittle failure (see Figure 1b–d). When openings along these cracks expose the warm underlying ocean to the frigid winter atmosphere, heat exchanges are large and local brine production increases as new ice grows and seawater freezes. Convergence or closing of pack ice forces the ice to raft or pile up into pressure ridges and to be forced down into keels, increasing the ice-ocean and ice-atmosphere drag. Typically, a distribution of openings and closings are formed when collections of ice floes with irregular boundaries are sheared relative to one another. Over time, the redistribution of ice associated with deformation alters the volume of sea ice and heat that can be stored within a given area of the Arctic Ocean. Together with thermodynamic

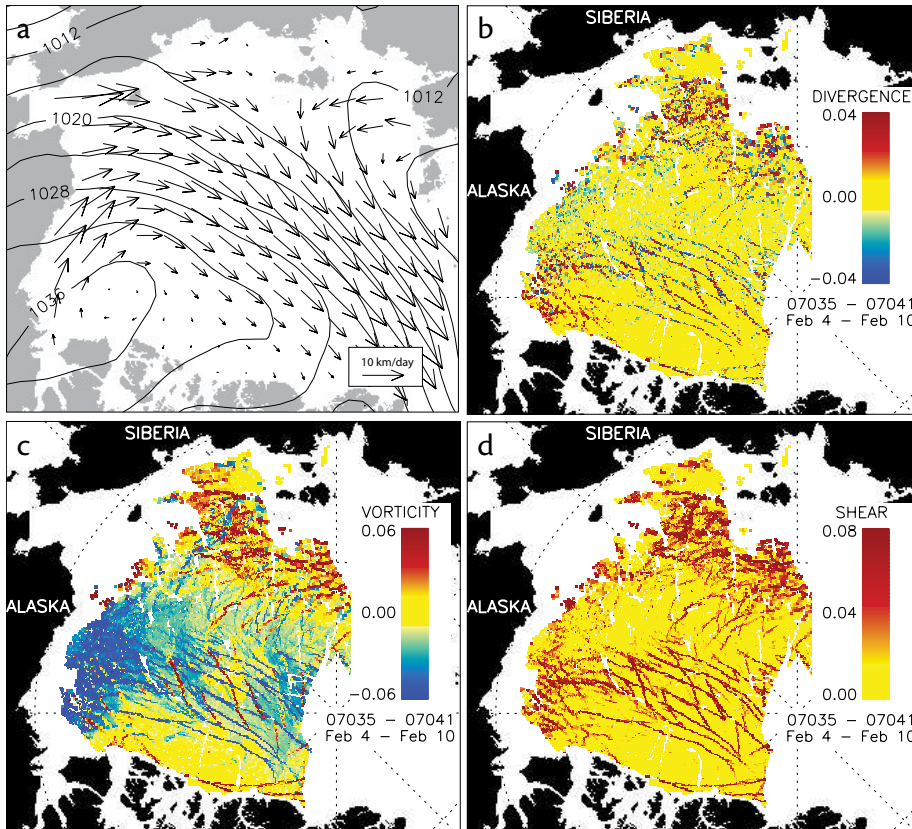


Figure 1. Large-scale mean ice motion and deformation of the Arctic Ocean ice cover between February 4 and February 10, 2007. The high-resolution ice deformation fields are derived from synthetic aperture radar imagery. (a) Mean vector field with superimposed sea level pressure contours (Interval: 4 hPa). (b) Divergence. (c) Vorticity. (d) Shear. Deformation computed at grid cell ~ 10 km on a side. Units: (/day).

growth, these dynamic processes shape the unique character of the ice cover's thickness distribution and profoundly impact the strength of the ice and its thermal properties over a wide range of temporal and spatial scales. Accurate quantification and simulation of the relative contributions of thermodynamics and dynamics to ice thickness distribution are thus crucial for understanding

Ron Kwok (ronald.kwok@jpl.nasa.gov) is Senior Research Scientist, Jet Propulsion Laboratory, California Institute of Technology, Pasadena, CA, USA.

Deborah Sulsky is Professor, Department of Mathematics and Statistics, University of New Mexico, Albuquerque, NM, USA.

the behavior and the vulnerability of the Arctic ice cover in a warming climate.

Measurement of small-scale sea ice motion is challenging because of the spatial and temporal scales spanned by the processes responsible for producing its variability. The relative motion between ice floes along narrow (meters to kilometers) fractures requires imaging sensors with not only high spatial resolution but also short sampling intervals. Ice deformation at subdaily time scales associated with tidal forcing or inertial effects are becoming more prominent as the ice cover thins. Presently, basin-scale fields of sea ice motion at different spatial resolutions can be derived from tracking common ice features in a variety of

satellite imagery (Emery et al., 1995). Of particular interest are those from satellite SAR imagery. SARs are uniquely suited for small-scale observations of sea ice cover because of their spatial resolution (tens of meters), their day/night coverage, and their ability to see through clouds. Temporal resolution, however, remains an issue because orbiting satellites are limited in their ability to cover the same area repeatedly. Thus, though subdaily sampling is currently not achievable, it remains an issue due to limitations of repeat coverage from orbiting satellites.

From 1997 to 2007, the SAR on RADARSAT (Canada's first commercial Earth observation satellite) provided routine three-day coverage of the Arctic Ocean for ice motion analyses. With the high-resolution sea ice kinematics (grid spacing of 5 km) from RADARSAT, we were able to approach the length and time scales appropriate for observing the expressions of smaller-scale sea ice processes. A joint project of the Alaska Satellite Facility and the Jet Propulsion Laboratory has been producing fine-scale sea ice motion products (Kwok, 1998) based on this data stream. The scientific objective of the project has been to provide a data set suitable for understanding the basin-scale behavior of small-scale sea ice kinematics on seasonal and interannual time scales, for improving ice dynamics in sea ice models, for documenting changes in sea ice, and for assimilation into coupled ice-ocean models.

The decade-long ice motion data set from this program allows a more detailed look at the small-scale, time-varying deformation of the ice cover (Kwok, 2001). The derived motion fields have been used to quantify the various

measures of opening, closing, and shear, and to estimate ice production and thickness. From analyses of these data sets, we are able to resolve and trace the development of these long, linear, fracture-associated features in the pack ice (Figure 1). The data set shows that the activity, persistence, orientation, and length scale of the fracture patterns are quite remarkable. The abundance of these quasilinear fractures is correlated to motion gradients and material strength, and they are organized into coherent patterns that persist for days. Contrast in the deformation shows that there are distinct differences in the deformation-induced ice production and in the density of these features in the seasonal and perennial ice zones (Kwok, 2006).

The dramatic changes in Arctic sea ice extent and thickness beg the question as to whether dynamics and thermodynamics act together to reduce ice mass or whether they have opposite effects. One could argue that since thin ice is more susceptible to ridging and that new ice is created in leads, deformation acts to increase ice thickness. On the other hand, it is possible that deformation causes the thinning ice pack to break apart more easily, and thermodynamic processes that ablate the ice are enhanced by this deformation. RADARSAT observations show that deformation-induced ice production in the seasonal ice zone is greater than 1.5 times that of the perennial ice zone. The younger seasonal ice is mechanically weaker; this observation points to a negative feedback mechanism where higher deformation and ice production is expected as the ice cover thins.

Differences between observations and

models are also notable. One examination of ice drift, export, deformation, deformation-related ice production, and spatial deformation patterns (Kwok et al., 2008) compares four coupled ice-ocean models with different attributes. The results show that even though the models are capable of reproducing large-scale drift patterns, variability among models is high. When compared to high-resolution kinematics from satellites, the shortcomings shared by the models are that: (1) the ice drift along coastal Alaska and Siberia is too slow, (2) the skill in explaining the time series of regional divergence of the ice cover is poor, and (3) deformation-related volume production is consistently lower. These discrepancies can be attributed to deficiencies in either the models or the forcing, but only occasionally (and not very often) can we find deformation patterns in models that resemble the linear features seen in satellite ice motion. Coon et al. (2007), upon reviewing available deformation and stress data, suggest that a model that includes deformation at discontinuities and an anisotropic failure surface would better describe the observed behavior of pack ice at shorter length scales. It is also evident that exact reproduction of these complex features would be costly and unnecessary. Thus, a relevant question is: how well should these patterns be simulated for improved climate simulations? High-resolution ice drift observations and coordinated field programs will be invaluable for answering this question as well as for future model development, improvements, and inter-comparisons, and especially for evaluation of the small-scale behavior of models with finer grid spacing.

SEA ICE THICKNESS

Two phenomena act to alter the thickness of floating ice. Thermodynamic processes are responsible for mass changes at the upper and lower surfaces of the ice, and mechanical processes, resulting from the nonuniform motion of the ice, cause the formation of leads and pressure ridges. If the ice cover did not deform, all of the ice in a particular climatic region would approach a uniform thickness predicted by thermodynamic equilibrium. The thickness distribution and photographs in Figure 2 illustrate the difference in character between the effects of thermodynamics and mechanics: on a yearlong average, the thermodynamics strives for a single equilibrium thickness (mode of the distribution) by net accretion to the thin ice and net ablation from the thick ice; in contrast, mechanics creates both open water and thick pressure ridges (in the tails of the distribution), thereby increasing local variations. Thermodynamics seeks the mean and mechanics the extreme. The thickness distribution is a time-integral of the interplay between these two processes (Thorndike et al., 1975).

Because of the importance of thickness in sea ice mass balance and in surface heat and energy budgets, remote determination of ice thickness at almost any spatial scale has long been desired. Existing satellite sensors, however, can see only radiation emitted or scattered from the top surface or the volume within the top few tens of centimeters of the ice and do not see the lower surface; this limitation is an obstacle to the direct observation of ice thickness. The current approach has been to use freeboard of the floating sea ice determined from

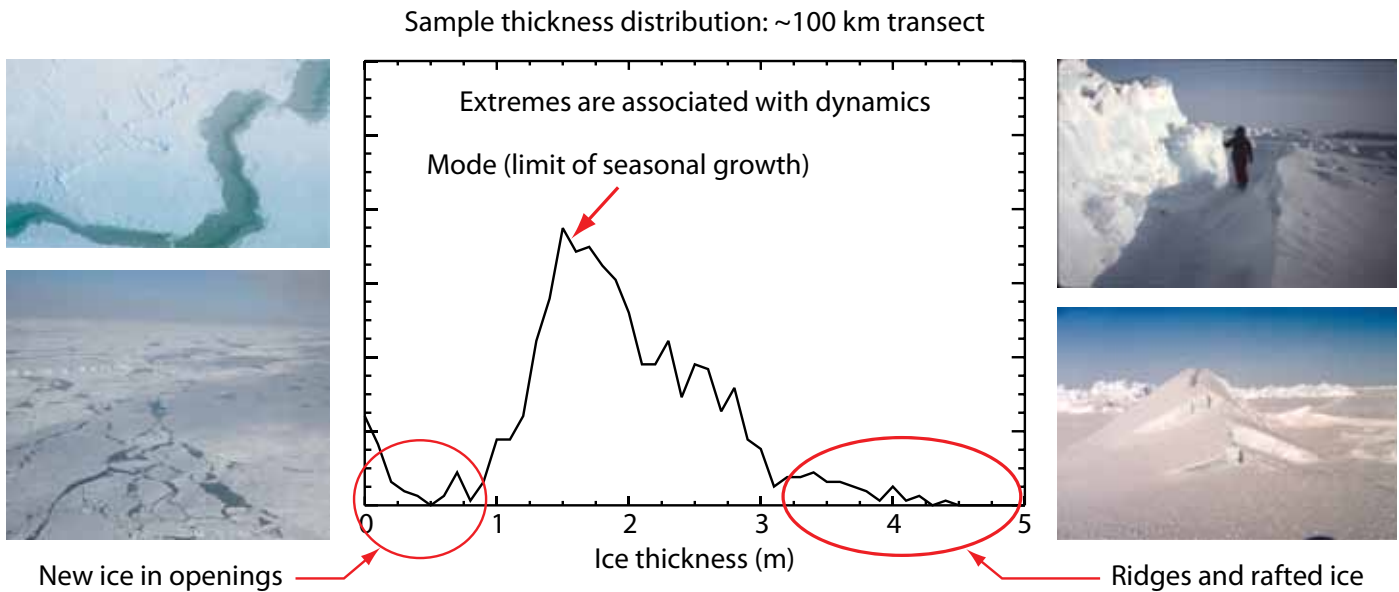


Figure 2. A sample sea ice thickness distribution from a 100-km profile illustrates the difference in character between the effects of thermodynamics and mechanics. On a yearlong average, thermodynamics strives for a single equilibrium thickness by net accretion to the thin ice and net ablation from the thick ice. In contrast, mechanics creates both thickness pressure ridges and open water.

altimeters, along with the assumption of hydrostatic equilibrium, to determine thickness. Freeboard is the elevation of the snow or ice surface above the local sea surface (Figure 3). The location of the measured surface from an altimeter (i.e., the air-snow or snow-ice interface) depends on whether the radiation transmitted penetrates the snow layer. To determine thickness, snow cover loading has to be accounted for. For lidars, because total freeboard is measured from the local sea surface to the air-snow interface, the snow loading is a larger source of uncertainty because only rough estimates of snow depth and density are available.

Present-day ocean and ice altimeters are able to provide the centimeter precision required for freeboard retrieval and thickness estimation. Laxon et al. (2003) describe the first geophysical results of ice freeboard and thickness estimates from spaceborne radar altimeters. Specular radar returns from open

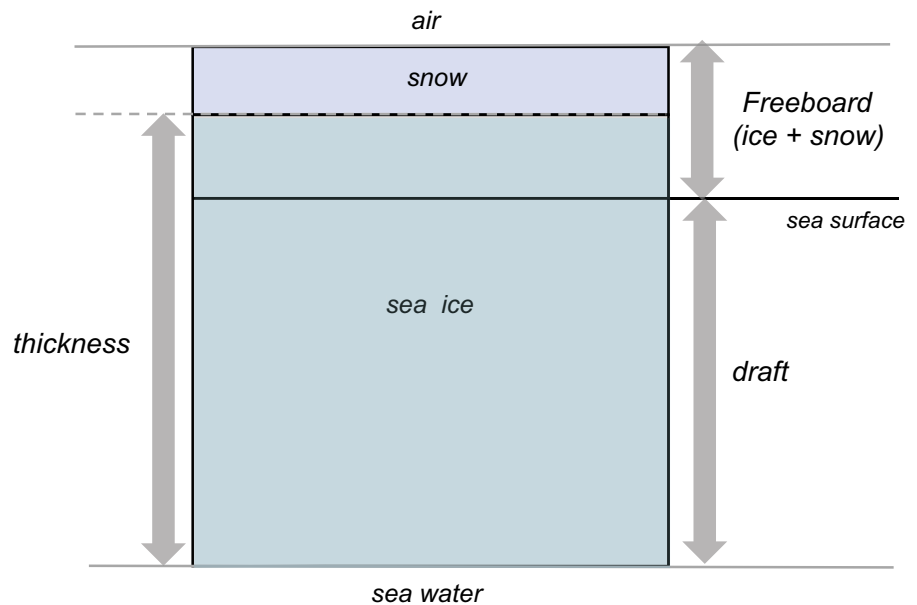


Figure 3. Schematic showing the relationship between total freeboard (snow + ice, sometimes known as surface height), draft, thickness, and the ocean surface. The current approach has been to use altimetric freeboard of the floating sea ice along with the assumption of hydrostatic equilibrium to determine ice thickness. Snow loading is obtained from snow depth from meteorological fields.

water or thin ice provide the necessary sea surface references for freeboard retrieval. Since 1993, the European Space Agency's (ESA's) European Remote Sensing (ERS) and Envisat satellite radar

altimeters have performed circum-Arctic observations south of 81.5°N. There is a data hole poleward of this latitude that covers approximately one-third of the area of the Arctic Basin. Envisat

observations between 2002 and 2008 suggest little change in thickness until early 2007, but a large decrease (25 cm) following the September 2007 ice extent minimum (Giles et al., 2008). However, this drop was regionally confined to parts of the Beaufort and Chukchi seas, and no significant changes were found in the eastern Arctic.

Recent work also demonstrated the feasibility of retrieving total freeboard and ice thickness from the lidar on the Ice, Cloud, and Land Elevation Satellite (ICESat) platform and documented the changes in Arctic sea ice thickness and volume (Kwok and Cunningham, 2008; Kwok et al., 2009). Even though ICESat data provided a near-basin-scale picture of Arctic sea ice thickness, temporal sampling was restricted due to laser life considerations. Over the duration of

the mission (2003–2009), only two to three 33-day campaigns each year were possible. As the ICESat orbit extended to 86°N, the data set provided better Arctic coverage than the radar altimeters and yielded observations of seasonal changes between winter and fall of each year. Data from 10 ICESat campaigns between 2003 and 2008 show rapid thinning and volume loss of the Arctic Ocean ice cover (Kwok et al., 2009). Comparison between radar- and lidar-derived ice thickness shows that, between 2004 and 2008, there is close agreement in the lower-latitude thinning south of 81.5°N between both data sets (Giles et al., 2008; Kwok et al., 2009).

Figure 4 shows the spatial patterns of sea ice thickness and the decline in basin mean thickness from ICESat during the five years from 2004–2008.

Overall, the gradient in the thickness fields across the Arctic follows a distinctive pattern, with the thickest multiyear ice (5–6 m) next to Ellesmere Island and the Greenland Coast, followed by a gradual thinning toward the central Arctic and the seasonal ice adjacent to the coasts of Alaska and Siberia. For the years shown in the figure, there was a remarkable thinning of about 0.6 m in multiyear ice thickness over four years along with a more than 42% decrease in multiyear ice coverage since 2005. In contrast, the average thickness of the seasonal ice in mid winter (~ 2 m), which covered more than two-thirds of the Arctic Ocean in 2007, changed negligibly. Average winter sea ice volume over the period, weighted by a loss of approximately 3000 km³ between 2007 and 2008, was about 14,000 km³. In the

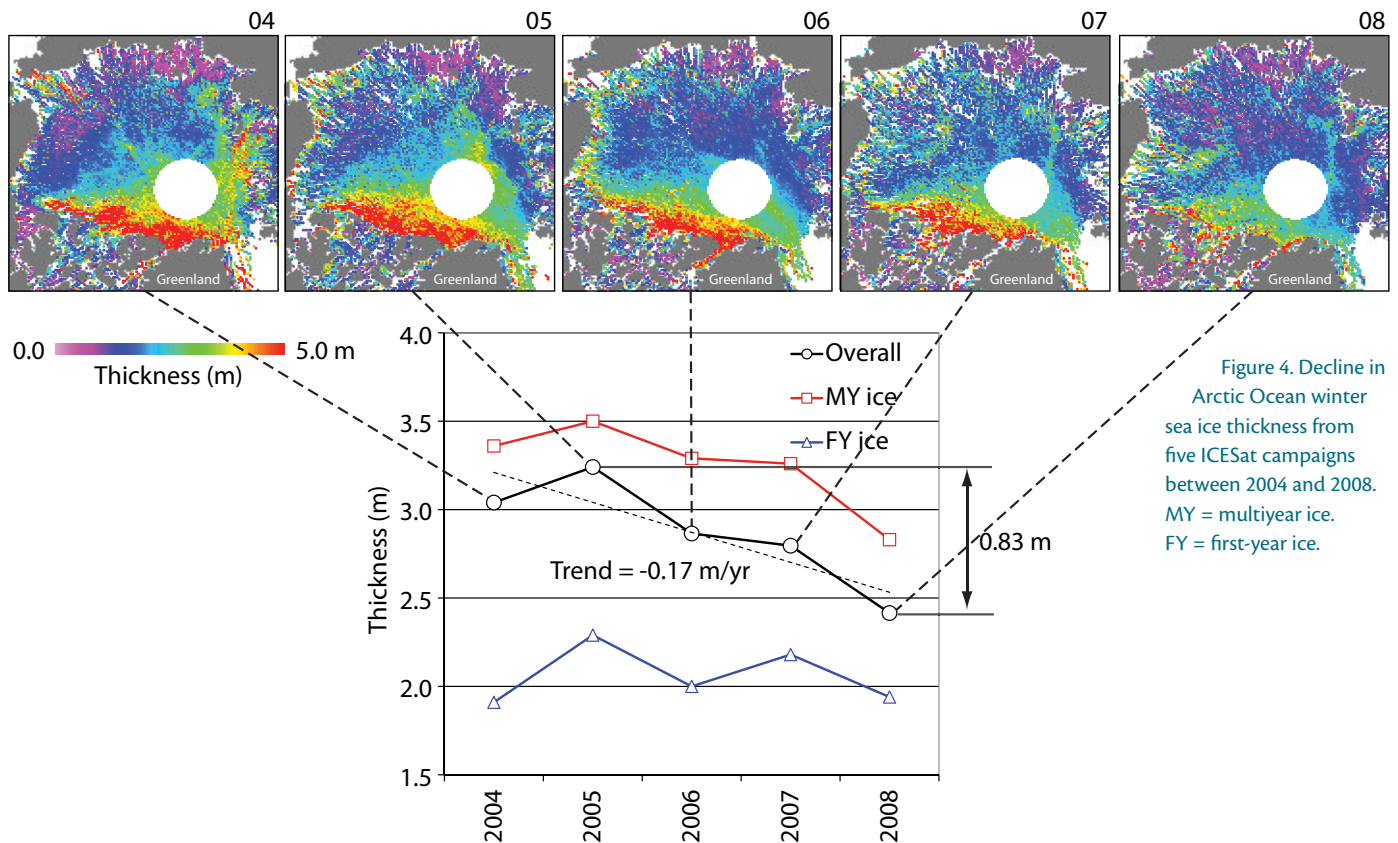


Figure 4. Decline in Arctic Ocean winter sea ice thickness from five ICESat campaigns between 2004 and 2008. MY = multiyear ice. FY = first-year ice.

four years since 2005, there has been a net loss in total multiyear ice volume of 6300 km³ (over 40%), while first-year ice cover gained volume due to increased overall area coverage. The data show that the overall declines in volume and thickness are explained almost entirely by changes in the multiyear ice cover. Combined with a large decline in multiyear ice coverage over this short record, there is a reversal in the volumetric and areal contributions of the two ice types to the total volume and area of the Arctic Ocean ice cover. Seasonal ice surpassed multiyear ice in winter area coverage and volume during these years. Assessment of the derived ice thicknesses shows that they are within 0.5 m of the estimates from submarines and moored upward-looking sonars.

This rapid decline in Arctic sea ice thickness and volume adds to the negative trend in ice area coverage over the past 30 years. Remote sensing during this period contributed significantly to our ability to monitor Arctic ice cover. The prospects of improving our observational capability during this decade will be addressed in the last section.

SEA ICE MODELING

Sea ice motion is governed by an equation describing the balance of momentum. This balance of momentum is an expression of Newton's Second Law that states: mass x acceleration = forces. Once the forces acting on sea ice are determined, acceleration is calculated. Acceleration is used to compute the current velocity, and then the ice moves in this velocity field. The forces acting on the ice are drag from the wind and ocean, Coriolis forces, gravitational effects from sea surface tilt, and internal

ice forces that follow a constitutive model. Drag laws are typically given by an adjustable coefficient multiplied by the square of the velocity difference between the ice and wind or ocean. These laws can be viewed as a parameterization of the more complicated physics embodied in the interaction between fluids and the ice structure.

Satellite observations have motivated many recent developments in constitutive modeling of sea ice. Early numerical simulations of sea ice motion assumed that cracks, leads, and ridges are randomly distributed over length scales in the range of 100 km (Coon, 1980). Under this assumption, ice behavior is described as isotropic, which is the only viable approach when computer resources limit the resolution available for more detailed calculations. However, observations show that fracture patterns in the Arctic are not randomly distributed. In a material with oriented fracture patterns, the material is weaker in strength across the fracture, yet it retains its strength along the fracture. When properties of a material depend on its orientation, an anisotropic model is more appropriate.

Although modelers have recognized for a while that the internal ice stresses are not isotropic (Thorndike and Colony, 1978), remote sensing has shown dramatically that leads are a dominant feature of the Arctic. In response, several anisotropic models (Coon et al., 1998; Hibler and Schulson, 2000; Wilchinsky and Feltham, 2004), as well as a model that describes damage formation in ice (Girard et al., in press), have been proposed to augment or replace the earlier plastic (Coon, et al., 1974) or viscous-plastic (Hibler, 1979)

model. In particular, Schreyer, et al. (2006) developed a model, called an elastic-decohesive model, to directly predict the initiation and opening of leads in Arctic ice. Once the mechanics of leads is taken into account through decohesion, the remaining ice motion has small deformations and is appropriately described as elastic. Decohesion describes the fracture process by reducing the traction on a presumed crack surface to zero over a small distance as the crack opens.

As ice moves, it can be mechanically redistributed through lead and ridge formation. Because computational grid cells are typically large compared to the horizontal scale over which ice thickness changes, thickness is parameterized by a thickness distribution (Thorndike and Maykut, 1973; Thorndike et al., 1975). The thickness distribution is the probability distribution of having ice of a given thickness in each computational cell. Thickness evolution is governed by the mechanical redistribution of ice plus growth and melt of ice as determined by the thermodynamics for a column of ice of each thickness. Thinner ice in the distribution increases when the ice motion diverges, and thinner ice can become thicker when the ice converges and ridges or keels form. The redistribution schemes are largely heuristic and difficult to verify empirically (Lipscomb et al., 2007). The thickness distribution is connected to dynamics because thickness affects ice strength.

For simplicity, temperature changes are computed for a vertical column of ice at each grid position on the ocean surface (Maykut and Untersteiner, 1961), for each thickness category in the thickness distribution. Thus, the

heat equation is solved in one space dimension and gives the temperature as a function of time in an ice column. Parameters in this equation are ice density (usually constant), heat capacity, and thermal conductivity. Heat capacity and thermal conductivity are functions of ice temperature and salinity. In more sophisticated models, these functions are adjusted to account for the presence of brine pockets (Bitz and Lipscomb, 1999). A fixed salinity profile through the ice thickness is usually assumed. Additionally, there is a heat source in the equation due to internal absorption of solar radiation that follows Beer's law. Interaction with the atmosphere and ocean is through heat flux boundary conditions. The balance of fluxes at the atmosphere-ice and ocean-ice interfaces determines whether ice melts or grows, changing its thickness.

Thus, sea ice models consist of three major components: the momentum equation governing ice motion, the heat equation governing ice thermodynamics, and the evolution of ice thickness distribution. In addition to motivating new constitutive models for sea ice, satellite observations provide a means to verify these model components. Figure 5a shows an example of the elastic-decohesive model used in conjunction with the material-point method (Sulsky et al., 2007) to solve the momentum equation for sea ice. The material-point method (MPM) identifies a set of material points in the ice initially and then tracks them throughout the deformation process. Each material point has mass, position, velocity, and stress, as well as any other material parameters and variables needed for the constitutive equation or thermodynamics. Six-hour wind fields

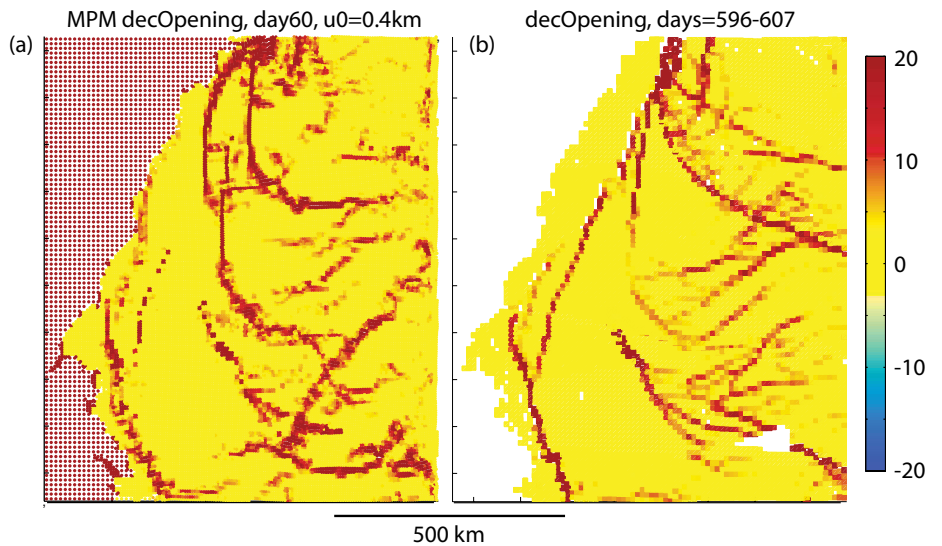


Figure 5. Opening displacement (leads) in the Beaufort Sea on March 2, 2004, computed (a) using the material-point method with the elastic-decohesive model and (b) kinematically using the RADARSAT Geophysical Processor System (RGPS) products. The color bar indicates the vector magnitude of the jump in displacement (i.e., both opening and shear displacement) divided by the scale factor $u_0=0.4$ km.

from the US National Weather Service National Centers for Environmental Prediction (NCEP) reanalysis are used to determine the wind drag. Ocean drag is determined from ocean currents updated daily from an ocean model (MITgcm; Marshall et al., 1997) run independently from the ice model. In addition to the momentum equation, a vertical heat equation based on the model of Bitz and Lipscomb (1999) is solved to determine the melting and freezing of ice, and an equation for the thickness distribution (Thorndike and Maykut, 1973), suitably modified to be consistent with the decohesive constitutive model, is also solved. The computational area for Figure 5a is an 831,600 km² region of the Beaufort Sea, and the time span is from February 23 to March 11, 2004. Each cell in the grid is colored by the amount of opening as computed by the elastic-decohesive model. The red areas are modeled leads

and the yellow areas are not deforming. For comparison, cells are colored similarly using a kinematic crack algorithm (Coon et al., 2007; Peterson and Sulsky, in press) to display the “observed” openings as shown in Figure 3b. Cell size in both the simulation and observations is 10 km. A model of this type shows promise in capturing the linear features and the finer-scale processes observed in satellite-derived data.

Because satellite observations cover a broad region, they provide an invaluable tool for assessing model performance. The broad coverage of satellite observations also makes it feasible to assimilate these data into numerical simulations and thus provide more accurate initial conditions for long-term climate predictions. Although the observed openings discussed above are derived from ice motion data obtained from satellite images, there is still more to be learned from ice thickness observations.

CONCLUSIONS AND OUTLOOK

The retrieval of sea ice thickness and small-scale motion from spaceborne imagery and altimetry is maturing, and its shortcomings are relatively well understood. During the last decade, separate observations of thickness and motion have provided new insights into the variability and changing processes

integrated response of the ice cover to a changing climate. It is also important to note that complementary field programs are essential for the assessment and verification of satellite retrieval procedures.

Unfortunately, the ICESat-1 mission has ended. ESA's CryoSat-2 was launched in April 2010. At an orbit inclination of 88°, the radar altimeter onboard will

aimed at providing an all-weather day-and-night supply of imagery. Sentinel-1 is to be followed by a second satellite a few years later.


Two NASA polar-orbiting missions (ICESat-2 and Deformation, Ecosystem Structure, and Dynamics of Ice [DESDynI]), both planned for launches this decade, are also tasked to address the observational needs of sea ice thickness and kinematics. One of the science objectives of ICESat-2 (launch date is late 2015) is to measure sea ice freeboard for estimation of sea ice thickness. The spacecraft will have a multibeam surface profiling lidar system (~ 10-m spots) for measuring sea ice freeboard. The DESDynI mission (launch is late 2017) will have an L-band SAR for imaging the Arctic Ocean as well as a multibeam lidar to provide routine observations of ice kinematics and freeboard over both the Arctic and Southern oceans. Combining a wide-swath SAR and a lidar system, this mission will provide fairly tightly coupled observations of ice kinematics and ice thickness. In terms of coverage, the ICESat-2 mission will provide lidar coverage up to 86°N while the DESDynI lidar will provide coverage to only 83°N. Both missions will provide near monthly mapping of Arctic Ocean ice freeboard and thickness within their coverage limit. The imaging radar on DESDynI will provide near-three-day mapping of sea ice kinematics.

During this decade, the prospects for improved satellite observation of Arctic Ocean sea ice are promising. The combined observations of thickness and kinematics will allow us to resolve the contributions of thermodynamics and dynamics to the ice thickness distribution for process studies and model

“ THE COMBINED OBSERVATIONS OF THICKNESS AND KINEMATICS WILL ALLOW US TO RESOLVE THE CONTRIBUTIONS OF THERMODYNAMICS AND DYNAMICS TO THE ICE THICKNESS DISTRIBUTION FOR PROCESS STUDIES AND MODEL IMPROVEMENTS, AND ALSO ALLOW US TO PROVIDE A DATA SET THAT IS SUITABLE FOR ASSIMILATION INTO GLOBAL MODELS. ”

inside the ice edge. These observations complement the multidecadal time series of ice extent from coarse resolution passive microwave sensors. The observations of kinematics and thickness have added to the understanding of the rapid decline of the ice cover during the last decade. Yet, the record of small-scale (kilometers) sea ice kinematics and thickness is short and incomplete due to coverage gaps and sensor issues. As thermodynamics and dynamics are related through their modification of the ice thickness distribution, there is a need for more extended and comprehensive observations of the coupled behavior of these parameters to understand their seasonal-to-decadal variability and the

provide continuous mapping of sea ice freeboard of a large fraction of the Arctic Ocean ice cover. Further, CryoSat-2 provides elevation estimates with improved spatial resolution of 250 m in the along-track direction using a synthetic aperture processing technique (Wingham et al., 2006). Currently, the Envisat altimeter and various imaging SARs are still active and are providing useful, though limited, coverage of Arctic ice cover. The Sentinel-1 European Radar Observatory, to be launched around 2012, is a polar-orbiting satellite system for the continuation of SAR applications, including observations of sea ice motion. It is a C-band imaging radar mission consisting of a pair of satellites

improvements, and also allow us to provide a data set that is suitable for assimilation into global models. 

ACKNOWLEDGEMENTS

RK performed this work at the Jet Propulsion Laboratory, California Institute of Technology, under contract with the National Aeronautics and Space Administration. DS was supported by the National Science Foundation under grant ARC-0621173.

REFERENCES

- Bitz, C.M., and W.H. Lipscomb. 1999. An energy-conserving thermodynamic model of sea ice. *Journal of Geophysical Research* 104(C7):15,669–15,677.
- Comiso, J.C. 2002. A rapidly declining perennial sea ice cover in the Arctic. *Geophysical Research Letters* 29(20):1,956, doi:10.1029/2002GL015650.
- Comiso, J.C., C.L. Parkinson, R. Gersten, and L. Stock. 2008. Accelerated decline in the Arctic sea ice cover. *Geophysical Research Letters* 35, L01703, doi:10.1029/2007GL031972.
- Coon, M.D. 1980. A review of AIDJEX modeling. Pp. 12–27 in *Sea Ice Processes and Models: Symposium Proceedings*. R.S. Pritchard, ed., University of Washington Press, Seattle, WA.
- Coon, M.D., G.S. Knoke, D.C. Echert, and R.S. Pritchard. 1998. The architecture of an anisotropic elastic-plastic sea ice mechanics constitutive law. *Journal of Geophysical Research* 103(C10):21,915–21,925.
- Coon, M., R. Kwok, G. Levy, M. Pruis, H. Schreyer, and D. Sulsky. 2007. Arctic Ice Dynamics Joint Experiment (AIDJEX) assumptions revisited and found inadequate. *Journal of Geophysical Research* 112, C11S90, doi:10.1029/2005JC003393.
- Coon, M.D., G.A. Maykut, R.S. Pritchard, D.A. Rothrock, and A.S. Thorndike. 1974. Modeling the pack ice as an elastic-plastic material. *AIDJEX Bulletin* 24:1–105.
- Emery, W., C. Fowler, and J. Maslanik. 1995. Satellite remote sensing of ice motion. Pp. 367–380 in *Oceanographic Applications of Remote Sensing*. M. Ikeda and F.W. Dobson, eds, CRC Press, Boca Raton, FL.
- Giles, K.A., S.W. Laxon, and A.L. Ridout. 2008. Circumpolar thinning of Arctic sea ice following the 2007 record ice extent minimum. *Geophysical Research Letters* 35, L22502, doi:10.1029/2008GL035710.
- Girard L., S. Bouillon, J. Weiss, D. Amtrano, T. Fichefet, and V. Legat. In press. A new modelling framework for sea ice mechanics based on elasto-brittle rheology. *Annals of Glaciology*.
- Hibler, W.D. III. 1979. A thermodynamic sea ice model. *Journal of Physical Oceanography* 9(4):815–846.
- Hibler, W.D. III, and E.M. Schulson. 2000. On modeling the anisotropic failure of flawed sea ice. *Journal of Geophysical Research* 105(C7):17,105–17,120.
- Integrated Global Observing Strategy. 2007. *Cryosphere Theme Report: For Monitoring Our Environment from Space and from Earth*. Integrated Global Observing Strategy, WMO/TD-No.1405, 100 pp. Available online at: cryos.ssec.wisc.edu/docs/cryos_theme_report.pdf (accessed September 23, 2010).
- Kwok, R. 1998. The RADARSAT Geophysical Processor System. Pp. 235–257 in *Analysis of SAR Data of the Polar Oceans: Recent Advances*. C. Tsatsoulis and R. Kwok, eds, Springer Verlag.
- Kwok, R. 2001. Deformation of the Arctic Ocean sea ice cover: November 1996 through April 1997. Pp. 315–323 in *Scaling Laws in Ice Mechanics and Dynamics*. J. Dempsey and H.H. Shen, eds, Kluwer Academic.
- Kwok, R. 2006. Contrasts in Arctic Ocean sea ice deformation and production in the seasonal and perennial ice zones. *Journal of Geophysical Research* 111, C11S22, doi:10.1029/2005JC003246
- Kwok, R., and G.F. Cunningham. 2008. ICESat over Arctic sea ice: Estimation of snow depth and ice thickness. *Journal of Geophysical Research* 113, C08010, doi:10.1029/2008JC004753.
- Kwok, R., G.F. Cunningham, M. Wensnahan, I. Rigor, H.J. Zwally, and D. Yi. 2009. Thinning and volume loss of Arctic sea ice: 2003–2008. *Journal of Geophysical Research* 114, C07005, doi:10.1029/2009JC005312.
- Kwok, R., E.C. Hunke, W. Maslowski, D. Menemenlis, and J. Zhang. 2008. Variability of sea ice simulations assessed with RGPS kinematics. *Journal of Geophysical Research* 113, C11012, doi:10.1029/2008JC004783.
- Kwok, R., and D.A. Rothrock. 2009. Decline in Arctic sea ice thickness from submarine and ICESat records: 1958–2008. *Geophysical Research Letters* 36, L15501, doi:10.1029/2009GL039035.
- Laxon, S., N. Peacock, and D. Smith. 2003. High interannual variability of sea ice thickness in the Arctic region. *Nature* 425:947–950.
- Lipscomb, W.H., E.C. Hunke, W. Maslowski, and J. Jakacki. 2007. Ridging, strength and stability in high-resolution sea ice models. *Journal of Geophysical Research* 112, C03S91, doi:10.1029/2005JC003355.
- Marshall, J., A. Adcroft, C. Hill, L. Perelman, and C. Heisey. 1997. A finite-volume, incompressible Navier-Stokes model for studies of the ocean on parallel computers. *Journal of Geophysical Research* 102(C3):5,753–5,766.
- Maykut, G.A., and N. Untersteiner. 1971. Some results from a time dependent, thermodynamic model of sea ice. *Journal of Geophysical Research* 76(6):1,550–1,575.
- Peterson, K., and D. Sulsky. In press. Evaluating sea ice deformation in the Beaufort Sea using a kinematic crack algorithm with RGPS data. In *Remote Sensing, Oceanic Manifestation of Global Changes*. D. Tang, J. Gower, K. Katsaros, G. Levy, R. Singh, and M.L. Heron, eds, Science Press/Springer.
- Polar Research Board. 2006. *Toward an Integrated Arctic Observing Network*. National Academies Press, Washington, DC, 116 pp.
- Schreyer, H.L., L. Munday, D. Sulsky, M. Coon, and R. Kwok. 2006. Elastic-decohesive constitutive model for sea ice. *Journal of Geophysical Research* 111, C11S26, doi:10.1029/2005JC003334.
- Sulsky, D.L., H. Schreyer, K. Peterson, M. Coon, and R. Kwok. 2007. Using the material-point method to model sea ice dynamics. *Journal of Geophysical Research* 112, C02S90, doi:10.1029/2005JC003329.
- Thorndike, A.S., and R. Colony. 1978. Estimating the deformation of sea ice. *AIJEX Bulletin* 37:25–36.
- Thorndike, A.S., and G.A. Maykut. 1973. On the thickness distribution of sea ice. *AIDJEX Bulletin* 21:31–48.
- Thorndike, A.S., D.A. Rothrock, G.A. Maykut, and R. Colony. 1975. The thickness distribution of sea ice. *Journal of Geophysical Research* 80(33):4,501–4,513.
- Wilchinsky, V., and D.L. Feltham. 2004. A continuum anisotropic model of sea ice dynamics. *Proceedings of the Royal Society of London A* 460:2,105–2,140.
- Wingham, D.J., C.R. Francis, S. Baker, C. Bouzinac, D. Brockley, R. Cullen, P. De Chateau-Thierry, S.W. Laxon, U. Mallow, C. Mavrocordatos, and others. 2006. CryoSat: A mission to determine the fluctuations in Earth's land and marine ice fields. *Advances in Space Research* 37:841–871.